

Activation of human visual area V6 during egocentric navigation with and without visual experience

Highlights

- V6 responds to visual egocentric navigation in humans
- V6 responds to both visual and auditory cues for navigation
- V6 is selective to egocentric navigation via sound, without any visual experience
- V6 receives sensory-motor input, which might play a role in egocentric navigation

Authors

Elena Aggius-Vella,
Daniel-Robert Chebat,
Shachar Maidenbaum, Amir Amedi

Correspondence

elenaaggiusvella@gmail.com (E.A.-V.),
danielc@ariel.ac.il (D.-R.C.),
mshachar@bgu.ac.il (S.M.),
amir.amed@idc.ac.il (A.A.)

In brief

Aggius-Vella et al. show that visual experience is not critical to develop selectivity for navigation in visual retinotopic area V6. People with blindness who learn to navigate virtual mazes based on a new sonification algorithm recruit area V6. Moreover, area V6 contains sensory-motor information that might be relevant for egocentric navigation.



Article

Activation of human visual area V6 during egocentric navigation with and without visual experience

Elena Aggius-Vella,^{1,*} Daniel-Robert Chebat,^{2,3,*} Shachar Maidenbaum,^{4,5,*} and Amir Amedi^{1,6,7,8,*}¹The Baruch Ivcher Institute for Brain, Cognition & Technology, Reichman University, 4610101 Herzliya, Israel²Department of Psychology, Faculty of Social Sciences and Humanities, Ariel University, 4076414 Ariel, Israel³Navigation and Accessibility Research Center of Ariel University (NARCA), Ariel University, 4076414 Ariel, Israel⁴Department of Biomedical Engineering, Ben-Gurion University of the Negev, 8410501 Beersheba, Israel⁵Zlotowski Center for Neuroscience, Ben-Gurion University of the Negev, 8410501 Beersheba, Israel⁶Twitter: @BCT_Inst⁷Twitter: @AmediLab⁸Lead contact*Correspondence: elenaaggiusvella@gmail.com (E.A.-V.), danielc@ariel.ac.il (D.-R.C.), mshachar@bgu.ac.il (S.M.), amir.amedil@idc.ac.il (A.A.)
<https://doi.org/10.1016/j.cub.2023.02.025>

SUMMARY

V6 is a retinotopic area located in the dorsal visual stream that integrates eye movements with retinal and visuo-motor signals. Despite the known role of V6 in visual motion, it is unknown whether it is involved in navigation and how sensory experiences shape its functional properties. We explored the involvement of V6 in egocentric navigation in sighted and in congenitally blind (CB) participants navigating via an in-house distance-to-sound sensory substitution device (SSD), the EyeCane. We performed two fMRI experiments on two independent datasets. In the first experiment, CB and sighted participants navigated the same mazes. The sighted performed the mazes via vision, while the CB performed them via audition. The CB performed the mazes before and after a training session, using the EyeCane SSD. In the second experiment, a group of sighted participants performed a motor topography task. Our results show that right V6 (rhV6) is selectively involved in egocentric navigation independently of the sensory modality used. Indeed, after training, rhV6 of CB is selectively recruited for auditory navigation, similarly to rhV6 in the sighted. Moreover, we found activation for body movement in area V6, which can putatively contribute to its involvement in egocentric navigation. Taken together, our findings suggest that area rhV6 is a unique hub that transforms spatially relevant sensory information into an egocentric representation for navigation. While vision is clearly the dominant modality, rhV6 is in fact a supramodal area that can develop its selectivity for navigation in the absence of visual experience.

INTRODUCTION

Visual information facilitates spatial tasks,¹ and it may even be required for the development of spatial abilities.^{2–4} It should therefore not be surprising that most of the brain regions associated with spatial tasks are also considered visual areas.^{5,6} Among these, the recently discovered area V6, located in the parieto-occipital sulcus (POS) and part of the dorsal visual stream, stands out for its retinotopic organization. V6 is organized in a topographic manner and includes representations of the entire contralateral hemifield,⁷ while playing a central role in integrating eye movements with retinal signals.^{8,9} Human and non-human primate studies show that area V6 is a motion area responding to coherent motion and to egomotion-compatible optic flow.^{9–14} V6 is activated by static but navigationally relevant stimuli, such as images of places (internal and external views of buildings),¹⁵ and it is connected with the parahippocampal place area

(PPA),¹⁶ suggesting that this area may possibly be involved in egocentric visual navigation. To the best of our knowledge, this is the first study testing the involvement of V6 in visual egocentric navigation tasks.

The classical view of typical brain development stresses the importance of an unalterable link between sensory cortices and their unisensory-specific experiences during the critical or sensitive periods, the time in early post-natal life during which the development of functional properties of the brain are strongly dependent on experience or environmental influences.^{17,18} However, an ever-growing body of evidence on brain organization in individuals who are congenitally blind (CB)^{19–27} and deaf^{28–31} suggests that in some cases, development of specializations and functions might not be completely dependent on visual or auditory (i.e., unisensory) input during the critical period. It can also be dramatically modified with tailored training in adulthood, even in the case of complete sensory deprivation starting



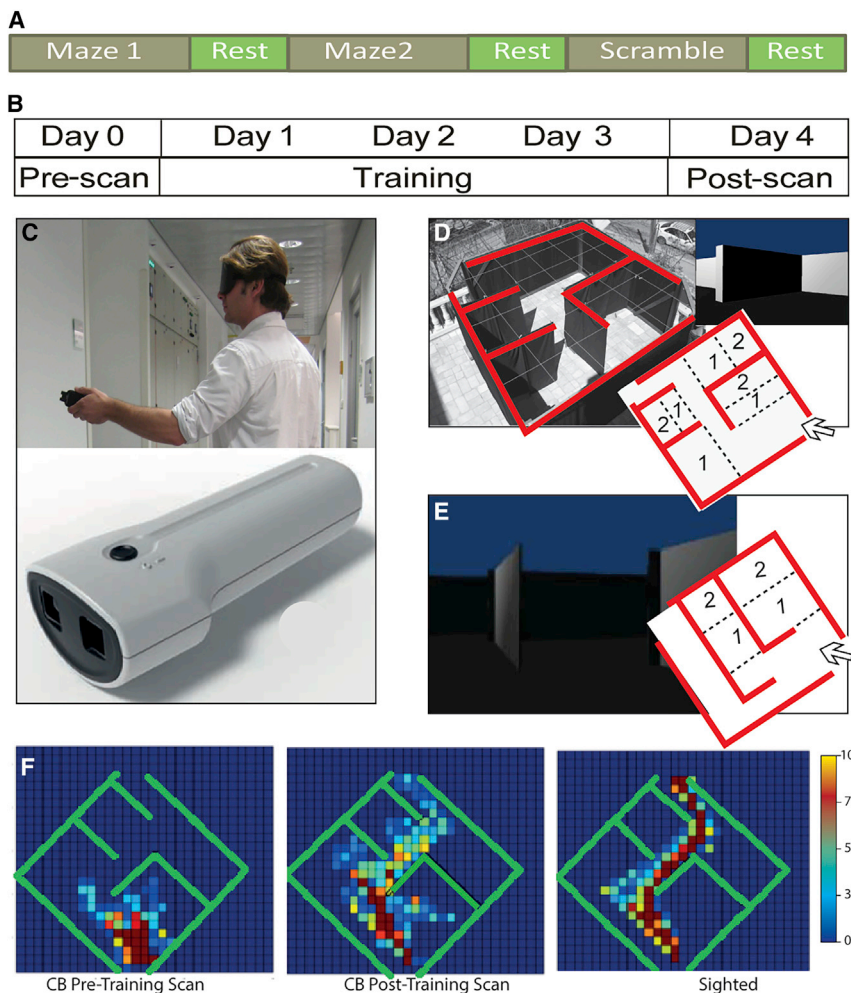


Figure 1. Sequence of tasks in fMRI experiments in virtual and real navigation training with the EyeCane

(A) The paradigm within the scanner; there were three types of blocks on which both groups were tested, while the training was performed only on one block and only by the blind group. The 3 blocks were maze 1 training (on which blind were trained), maze 2 no training (on which blind were not trained), and a scrambled task (used as control task). Each block was repeated 4 times per run, and there were 2 runs on each scanning day.

(B) The experimental protocol consisted of a pre-training fMRI scan, followed by 3 days of training in both real and virtual environments and a post-training scan.

(C) The EyeCane device, a unique visual to auditory sensory substitution device (SSD) that maps distance information into sounds.^{54,92}

(D) Setup of maze 1 training; numbers correspond to errors rate and are based on deviance from the correct path.

(E) Setup of the novel maze 2 no training; numbers correspond to errors rate and are based on deviance from the correct path.

(F) Heatmaps of the path taken by the CB pre-training, CB post-training, and sighted groups in maze 1 training during the scan for each of the groups. The heatmap represents the amount of time spent by each participant in the different areas of the maze for both the PRE (pre-training) and POST (post-training) conditions. The time spent in each point was defined by calculating the time between 2 key strokes (a key stroke represents a step), see [STAR Methods](#). Hotter colors indicate that on average, participants in that group spent more time in that location. The heatmaps show that in the post-training condition, the blind participants were able to find the exit to the maze similarly to the sighted.

in the first years of life.^{20,32–38} Despite the visual nature of area V6, it is unknown whether its task specialization can develop in the absence of visual experience. This question is even more intriguing since CB individuals can perform spatial tasks, using tactile or auditory cues,^{20,22,33,38–40} as well as sighted participants using vision^{22,38,41} or can even outperform them in certain navigation tasks by using sensory substitution devices (SSDs).³³ First, we tested if area V6 is selectively recruited in a visual navigation task. Our results show that area V6 of the sighted exhibits a higher response to navigation tasks, compared with the control condition. Second, given the involvement seen here of V6 in visual egocentric navigation tasks, we wanted to explore whether visual experience, during development, is necessary for the functional specialization of V6 for navigation tasks. To this end, we compare activations in V6 for egocentric navigation information, delivered via auditory feedback in the CB, with activations in V6 for egocentric navigation information, delivered via vision in sighted individuals.

Animal^{42–44} and human studies^{13,15} show that V6 is involved in processing visual motion in relation to body and eye-centered reference frames.¹³ It is suggested that V6 is involved in “subtracting out” self-motion signals across the whole visual field, as well as in providing information about moving objects and

their relative distance.^{11,45} Research on monkeys^{44,46,47} shows an indirect connection between area V6 and the premotor cortex by describing the flow of the visual pathway to the frontal cortex in 4 cerebral stations: V1 → V6 → V6A/MIP → dorsal area 6. Studies on humans replicated these findings¹⁶ and added a functional differentiation between area V6 and V6A. Thus, it seems that area V6 processes motion of objects in the depth dimension, translating and adapting this information to self-motion cues. This information is conveyed to V6Av for the evaluation of object distance in relation to the dynamic self-motion.^{13,16,48} Based on these characteristics, and the fact that V6 seems dedicated to processing spatial distance based on body position,^{16,49} it is plausible that this area is a suitable candidate for the processing of egocentric visual navigation, i.e., the representation of space based on body position.^{7,15,48,50,51} We therefore also investigated whether V6 responds to body movements.

We performed two separate experiments. In the first, both sighted and CB individuals underwent fMRI while they were navigating in first-person perspective two different virtual versions of the classical Hebb-Williams (HB) mazes ([Figure 1](#)), a set of mazes used to test cognitive ability in humans and animals. Both the sighted and the CB performed the same two-maze navigation task and a (scrambled) control condition. The sighted group

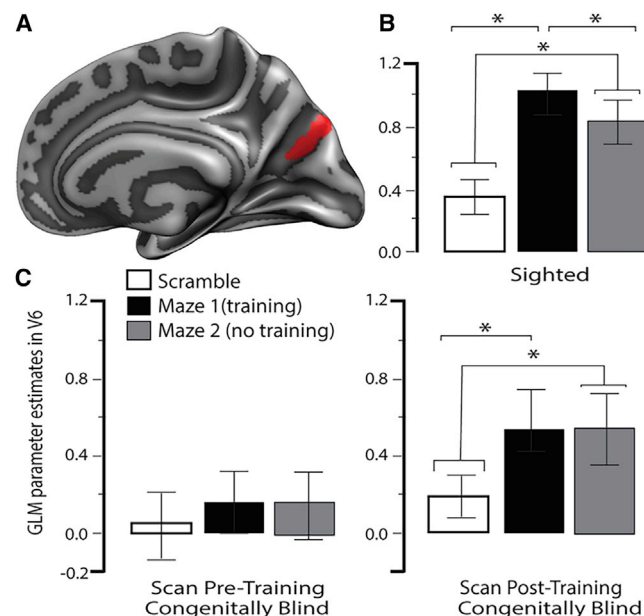


Figure 2. V6 is selective for navigation

(A) V6 location is shown in red, and its extension is defined through alignment of participants' brains to the Glasser atlas.
(B) Area V6 is selective for navigation task in the sighted group.
(C) Area V6 is recruited during auditory navigation task in blind participants, but it begins its selectivity only after the training. Error bars denote the SEM. See also Figure S1.

navigated by using full vision. They received also auditory input from the EyeCane, whereas the CB group received only auditory input from the EyeCane, an SSD that allows the user to scan the environment through hand movements, mimicking eye movements and converting visual distance information into auditory feedback⁵²: the further away the wall was, the lower was the frequency of the sound (Figure 1C). The 2 HB mazes used are similar in terms of length and difficulty. Participants used the keyboard to navigate with the aid of the EyeCane SSD and received visual or auditory information about the environment through the device. In the (scrambled) control condition, participants were instructed to navigate randomly in different directions by pressing the arrow keys. In this condition, the auditory and/or visual cues were “scrambled,” meaning that they were not informative of their movements in the environment. The CB underwent two scanning sessions, once before and then again after a training session in which CB participants navigated in both the real and virtual Hebb-Williams mazes. Training in the maze was spread out over a 3-day period (Figure 1B). Similarly to methods used in animals studies,^{54,55} participants were trained only on one Hebb-Williams maze, here called “maze 1 training” (Figure 1D), while the untrained Hebb-Williams maze, here called “maze 2 no training” (Figure 1E), was used as a control condition to check training generalization (Table S1). Results show that V6 of the sighted group responds selectively to the maze conditions, suggesting its role in navigation. Before the training, V6 of the CB does not respond to auditory navigation cues, and this was expected as it had not developed its specialization, neither via vision nor audition. After the training session

with an auditory device that enables them to navigate, V6 of CB participants is recruited to selectively process auditory navigation cues.

RESULTS

Experiment 1: Area V6 is selectively recruited in visual navigation tasks for the sighted

During fMRI, fourteen sighted participants performed the HW mazes navigation task and the scrambled condition (see STAR Methods), using vision and the auditory navigation input from the EyeCane device (see STAR Methods). Regional generalized linear model (GLM) analysis was applied to anatomical areas V6 (Figure 2A), defined by the Glasser atlas,⁵⁶ an atlas defined by sharp changes in cortical architecture, function, connectivity, and/or topography in a precisely aligned group average of 210 healthy young adults. We did not use a functional localizer as it could not be run in the CB. Moreover, it is known that there is high variability in retinotopic maps in V6 across participants, therefore a localizer defined only on our sighted sample could not take into account such variability. For this reason, we used the Glasser atlas that can consider inter-individual variability as it is based on topography from a group of 210 people. The V6 regions identified by Glasser and Pitzalis overlap to some extent, but it is unclear whether they represent the same area. Glasser's V6 appears to be larger than Pitzalis's retinotopically defined V6 and is more similar to V6+, which may include a portion of V6A.^{45,57} Specific experiments are needed to verify this point. Results from the right hemisphere of the sighted group show higher activations for both navigation conditions, i.e., the two mazes versus the scrambled condition ($t_{(13)} = 5.2$, $p < 0.001$) and ($t_{(13)} = 3.2$, $p = 0.01$) (Figure 2B), and different activations were also reported between the two navigation conditions ($t_{(13)} = 2.4$, $p = 0.03$). Beta probability map from the same contrast confirms a consistent involvement of area V6 in navigation (Figure S1). Left (lh) area V6 was also selectively recruited for navigation conditions ($t_{(13)} = 4.5$, $p = 0.002$) and ($t_{(13)} = 3.7$, $p = 0.004$), while no differences were reported between the two mazes.

Area V6 can develop its specialization for navigation even in the absence of visual experience from birth

Nine CB participants used the auditory input from the EyeCane to perform the same three navigation conditions performed by the sighted. The three auditory navigation conditions were repeated before and after a training session with the EyeCane (3 training sessions were spread out over a period of 3 days. Each session lasted about 2 h in both real and virtual mazes (Table S1). Results indicate that before training, both left and right V6 areas of the CB were not responsive to navigation auditory cues across participants (as shown in Figures 2C and S1). However, after training with the EyeCane, the right V6 of the CB group began to selectively respond to both maze 1 training ($t_{(8)} = 3.2$, $p = 0.03$) and maze 2 no training ($t_{(8)} = 2.6$, $p = 0.04$) conditions, compared with the scrambled condition. There were no differences in activation between mazes ($p > 0.05$) (as shown in Figure 2C). The recruitment of V6 for navigation in the post-training session is consistent across participants (Figure S1). Our findings suggest that V6 has an amodal/supramodal

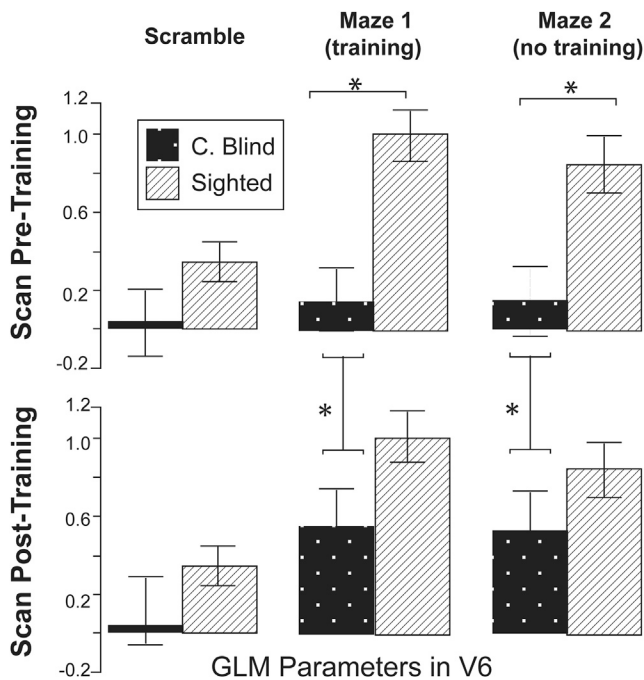


Figure 3. Sensory learning in specific task

Upper row: strong differences in activation between sighted (white with black stripes) and blind (black with white dots) participants before training on navigation with the aid of EyeCane. This difference strongly supports the specificity of V6 in navigation conditions. After training (lower row), rhV6 of congenitally blind participants develops its specialization for navigation task, reaching selectively confined to both mazes (1 training and 2 no training) but not scrambled condition. Importantly, this result suggests a sort of task-specific rewiring of audition in visual cortex, as the effect is generalized to the maze 2 no training maze too. Error bars denote the SEM.

See also Figure S1.

organization, which may be task-specific sensory-independent (TSSI) organization. This organization may explain the long-term plasticity of V6, including the reopening or extension of the critical period for different sensory modalities. No differences between conditions were reported in the left hemisphere.

Area V6 can learn to respond to auditory navigation cues in congenitally blind individuals

We compared the performance of the CB with that of the sighted for both the pre- and post-training conditions. This analysis reveals that before training, rhV6 activation differs between the two groups in both navigation conditions—for the maze 1 training ($t_{(21)} = -4$, $p < 0.001$) and the maze 2 no training ($t_{(21)} = -3.2$, $p = 0.007$)—but crucially, no difference was reported for the scrambled condition ($p > 0.05$) (Figure 3, upper row). However, after training, area rhV6 of the CB reached similar activation levels of rhV6 than the sighted in all tested conditions: maze 1 training ($t_{(21)} = -2$, $p > 0.05$), maze 2 no training ($t_{(21)} = -1.3$, $p > 0.05$), and the scrambled condition ($t_{(21)} = -1$, $p > 0.05$) (Figures 3 [lower row] and S1).

Analysis of the learning observed between the pre- and post-training conditions (post > pre) (Figure 3, black with white dots, bars across rows) showed a selective consistent increase of rhV6 activation in the navigation conditions: maze 1 training

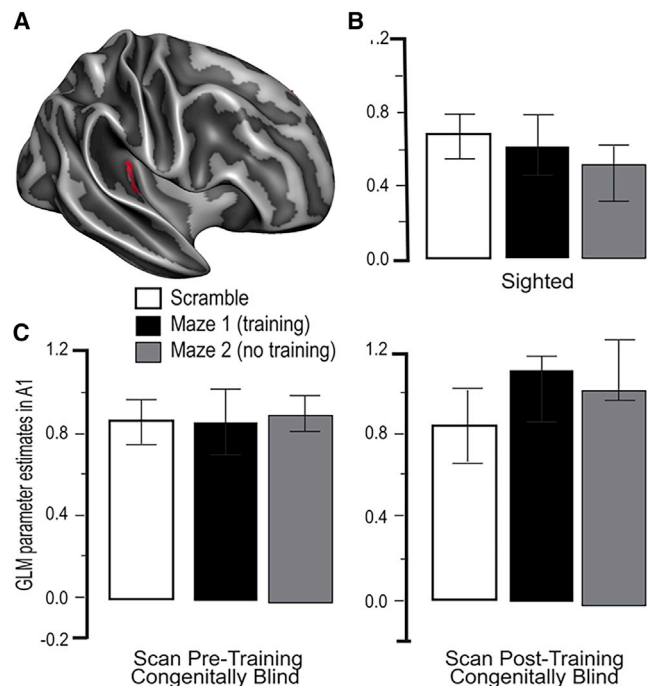


Figure 4. Auditory cortex

(A) A1 location is shown in red and its extension is defined through alignment of participants' brains to the Glasser atlas.

(B and C) No differences between conditions in A1 of sighted (B) and of blind (C) participants in both sessions.

Error bars denote the SEM.

($t_{(8)} = -4.1$, $p = 0.005$) and maze 2 no training ($t_{(8)} = -4.5$, $p = 0.005$), while no learning effect is shown in the scrambled condition ($t_{(8)} = -1.2$, $p > 0.05$). No differences between conditions were reported in the left hemisphere ($p > 0.05$). These findings are congruent with the behavioral results outside of the scanner,^{38,41} showing an improvement in performance after navigation training.

Effect of training is confined to rhV6 and does not affect other areas stimulated by the task

To investigate if the learning effect in the POS was specific to V6 and did not affect other areas stimulated by our paradigm (like the auditory cortex) not dedicated to navigation, we performed a regional analysis in area A1. Results show no differences ($p > 0.05$) within groups and between sessions (Figure 4). The result of this analysis is important because it confirms there are no difference in auditory cues between the 3 conditions in the auditory cortex. Furthermore, the visual areas that are located adjacent to area V6, namely, area V6A and DVT, did not show the learning effect ($p > 0.05$) for navigation via sounds. Rh DVT showed no differences between conditions in the pre-training session, whereas in the post-training session, it showed higher activations for both mazes, compared with the scrambled condition: maze 1 training ($t_{(8)} = 3.9$, $p = 0.01$) and maze 2 no training ($t_{(8)} = 2.8$, $p = 0.03$). No differences were reported in the left hemisphere. Rh V6A did not show any difference between both mazes and the scrambled condition, neither in the pre-training nor post-training session ($p > 0.05$). LH V6A shows no

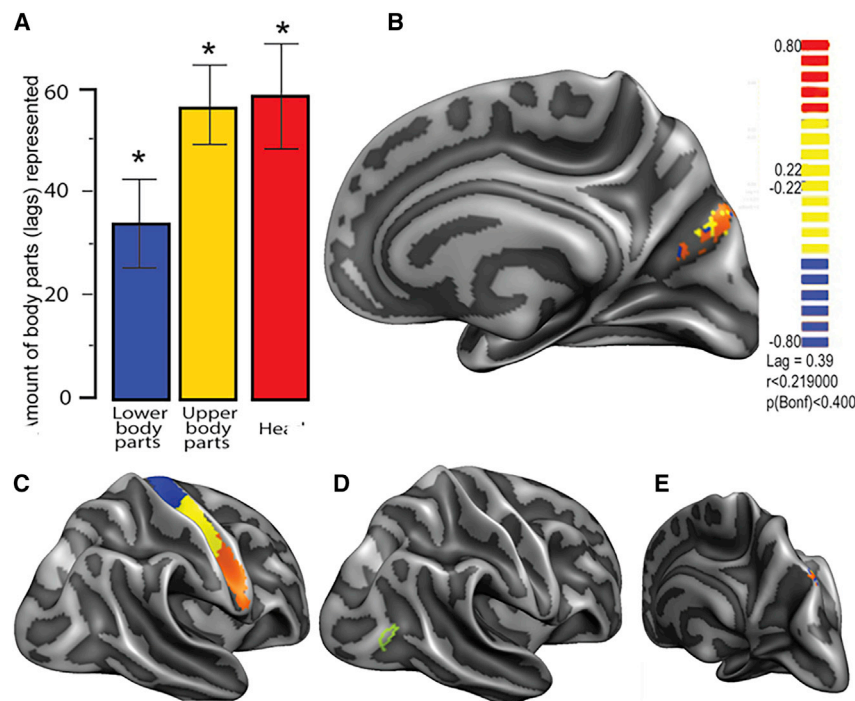


Figure 5. Body representation in V6

(A) The column plot shows the amount of vertex activated by each body part/lag. T test versus 0 showed a full body activation inside V6 (stars above each bar). The plot shows that most of the significant voxels are from the head and upper body parts. Error bars denote the SEM.

(B) Area V6 is activated by body movement. Red colors correspond to the head, yellow to the upper body parts, and blue to the lower body parts. Every color in the bar plot represents a different body part (head: red, upper body parts: yellow, lower body parts: blue), the statistical threshold used, and the related statistic. Since our design here was of periodic, phase locking design—each phase corresponded to a given body (see Zeharia et al.^{93–95}).

(C) Somatotopic motor homunculus in area 4.

(D) Lack of motor information in area MT, visual motion area that responds to object movements⁴⁵ and to both coherent and incoherent optic flow.

(E) Body motor activation in area V6A, an area that integrates eye and hand movements for reaching.

differences between conditions before training ($p > 0.05$). After training, the left V6A area had more activity for both mazes, compared with the scrambled condition: maze 1 training ($t_{(8)} = 2.0$, $p = 0.03$) and maze 2 no training ($t_{(8)} = 2.8$, $p = 0.03$).

Experiment 2: First-person perspective may require body motor information

During fMRI, 19 sighted participants performed a motor task in which they moved 20 body parts consecutively in a fixed order (see STAR Methods). Full-brain cross-correlations allowed us to identify voxel-vertices responding to specific body part movements. The 20 body parts were grouped into 3 sections: head, upper body (including arms), and lower body (including legs), based on anatomical topography (see STAR Methods). This analysis shows that in the more dorsal part of area V6, there are voxels activated during movement of each body section ($p < 0.05$) (Figure 5B). Results show that a higher number of vertices responded to the head and upper body parts (shown as red and yellow, respectively, in Figures 5A and 5B), when compared with the lower body parts (shown in blue). Importantly, another key area for visual motion, i.e., area MT (Figure 5D), does not show any body information. These results suggest that brain areas dedicated to tasks involving the body may be the only areas that contain information about body movements. In this study, area V6 appears to represent spatial information based on the body's position. To support this hypothesis, we performed the same analysis on 2 additional areas involved in motor tasks. Figure 5C shows the homunculus in motor area 4, and Figure 5E shows the motor activation in area V6A that it is involved in eye-hand coordination for reaching.^{61,62} Topographic analyses of areas 4, V6, and MT revealed a well-defined somatotopic map in area 4 and very broad tuning in area V6 with a preference for the upper body, while MT (which served as a control visual

motion area) seems not to be activated significantly by body movements. Taken together, our results suggest that even in the case of complete visual deprivation from birth and during the critical period, area V6 can develop the same functional specialization for navigation via the auditory modality. We show that V6 can be recruited to respond to auditory cues, providing egocentric spatial information for navigation after a short training session. The body motor activation, with a preference for the head, found in area V6 sheds new light on the function of area V6, suggesting that it is a part of the egocentric reference frame network. Future work should investigate the role of different body parts in area V6 and their direct contribution to egocentric navigation.

DISCUSSION

V6 is a motion-sensitive area that mostly represents the peripheral part of the visual field^{7,10,63} and is responsive to translational motion.¹⁰ Macaque V6 includes many real-motion neurons, and it responds to coherent motion and to egomotion-compatible optic flow.^{9–12,64} It has been suggested that it is involved in object-motion recognition¹³ and in processing spatial distance cues based on body position.^{16,49} V6 plays a central role in integrating eye movements with retinal signals^{8,65,66} and is involved in processing visual motion in relation to body and eye reference frames.^{13,14} Based on this evidence, previous reports hypothesized that area V6 can be selectively involved in egocentric navigation tasks. This hypothesis aligns with previous findings, regarding the connectivity between area V6 and the PPA,¹⁶ showing that area V6 is activated by static but navigationally relevant stimuli, such as images of places (internal and external views of buildings).¹⁵ Based on this, we first tested the role of area V6 in a visual egocentric navigation task. Our results show that area V6 is selectively recruited during visual egocentric navigation and that its sensory organization can develop even in the absence of visual experience from birth.

After a short training period with the EyeCane SSD, we found activation in the dorsal part of the POS of the CB group that mainly includes V6 and maybe minor parts of the nearby V6A and DVT. Indeed, the post-training activation in V6 of the CB is similar to what is found in V6 of the sighted. In a second separate experiment, we explored whether V6 also responds to sensory-motor movements, given the nature of egocentric navigation. To this end, we applied phase locking methods to a motor topography task. We found that area V6 can encode body motor information with a preference for the upper body parts.

Additionally, area rhV6 of CB individuals becomes selectively recruited to process auditory navigation cues, reaching activation levels similar to those observed in rhV6 of the sighted group, navigating by using vision, and with similar selectivity patterns in exactly the same HW mazes. This result suggests that by replacing visual information with auditory cues, it is possible for V6 to be selective for egocentric navigation. This finding challenges the notion that brain plasticity in V6 is limited by critical periods, and it instead supports the idea that the brain is organized in a supramodal manner, with selective specialization for specific tasks or functions that can be developed later in life with the right training or technologies.^{20,32–38} The sensory-independent (or supramodal) organization of area v6 was already evident in the pre-training session. Blind and sighted individuals did not differ on the scrambled condition but only on the navigation conditions in this area. This result strongly supports the idea that activation in area V6 is not influenced by the nature of the sensory modalities but rather specifically by the task-specific information that they convey. In line with findings showing TSSI organization in both the ventral^{67–71} and dorsal visual streams,^{24,26,27,72} we provide new evidence supporting our hypothesis that V6 is also organized in a TSSI/amodal/supramodal fashion. Furthermore, our data suggest that rhV6 can also learn and generalize auditory spatial distance information in relation to body motion cues. The recruitment of rhV6 by auditory cues, conveying information about distance from the body, in the post-training conditions supports the idea that the critical period for V6 can be reversible.

We did not find evidence of task-related changes in the left hemisphere during navigation. This fact is in line with an abundance of literature showing the predominant role of the right hemisphere in spatial/navigation tasks.^{73,74} For example, a study on patients⁷⁵ who were implanted with intracranial electroencephalographic recordings shows activation lateralized to the right hemisphere, especially in posterior neocortex during a virtual navigation task. Specifically, they found right-lateralized gamma oscillations during a virtual spatial-navigation task. It is well known that in humans and other animals, gamma oscillations are a general marker of local neuronal activation and often indicate that information is being exchanged between brain regions.^{76,77} Moreover, the fMRI BOLD signal correlates with gamma-band EEG oscillations in neocortex recordings from humans and non-human primates.^{78–80} However, we cannot completely exclude the possibility that a methodological or other limitation leads to overemphasizing the lateralization found in the CB.

Finally, we show that area V6 is activated by the body motor task with a preference for the movements of the upper body parts, while lower body parts showed the least activation (but see Serra et al. and Pitzalis et al.^{57,81} who did not find such

activation). We speculate that this novel yet preliminary result can be related to the selective activation of area V6 for egocentric navigation tasks. We suggest that area V6 could use an eye/head centric reference frame. The interpretation of our results is supported by studies that showed that area V6 codes space based on eye and body position and on self-motion.^{13,14} However, the topic is still under debate, and future experiments are needed to test the presence and role of sensory-motor input in V6.

It is important to note that area MT (Figure 5D), a motion area functionally similar to V6, does not show any body-related activations. We suggest that this difference can be explained by the fact that area MT responds to object movements,⁴⁵ and so to both coherent and incoherent optic flow, whereas area V6 is more selective to coherent motion, the same motion produced by self movement.^{10,13,14} In this study, the region of activation is compared with sighted regions of interest (ROIs) that are derived from many participants. However, important inter-individual variability was reported in terms of the location of these two retinotopic visual areas V6 and V6A. Due to this, we cannot exclude that area V6, as defined by the Glasser atlas, could include parts of V6A and that this could lead to a bias in the lack of left V6 sensory reorganization. However, Glasser V6 and V6A are very close to areas V6 and V6A, as defined by Pitzalis et al.^{48,61}

In conclusion, our findings suggest that V6 is a unique hub within which audio, visual, and body information are analyzed to drive online body movement in space. We^{24,82,83} and several other labs^{72,84–86} have recently shown that high-order visual category-selective areas can develop their functions even without visual experience during critical periods, which are defined as a time window early in life during which sensory cortices (e.g., visual cortex) must be exposed to their unisensory stimulus (e.g., visual input) in order to establish the corresponding activity and behavior (e.g., category selectivity to objects, faces, etc.). Our recent results show that such category selectivity can develop even without any visual experience. However, to the best of our knowledge, this study is the first to show that a retinotopic area such as area V6 can develop selectivity to egocentric navigation in the absence of visual experience. This is surprising because retinotopic areas have been shown to be extremely sensitive to visual experience during development,^{87–91} so the present results challenge the limits of critical periods for the functional development of V6.

Limitations of the study

Important inter-individual variability was reported in terms of the location of these two retinotopic visual areas V6 and V6A. Due to this, we cannot exclude that area V6, as defined by the Glasser atlas, could include parts of V6A and that this could lead to a bias in the lack of left V6 sensory reorganization. The region of activation in the present work is compared with sighted ROIs that are derived from many participants. So, the possibility that it includes, at least partly, V6A in addition to area V6 should be considered. This work shows that V6 contains voxels responding to movements; however, further research is needed to explore the role of eye movements inside area V6 and the exact role of this motor activation in egocentric navigation tasks.

This study cannot rule out the possibility that the body map found in area V6 supports other, unrelated mechanisms.

STAR★METHODS

Detailed methods are provided in the online version of this paper and include the following:

- **KEY RESOURCES TABLE**
- **RESOURCE AVAILABILITY**
 - Lead contact
 - Materials availability
 - Data and code availability
- **EXPERIMENTAL MODEL AND SUBJECT DETAILS**
- **METHOD DETAILS**
 - Navigation task
 - The virtual navigation setup
 - Body motor task
- **QUANTIFICATION AND STATISTICAL ANALYSIS**
 - Navigation task
 - Navigation task. Regions of interest (ROI) analysis
 - Body motor task
 - Body motor task ROI mask
 - Both experiments

SUPPLEMENTAL INFORMATION

Supplemental information can be found online at <https://doi.org/10.1016/j.cub.2023.02.025>.

ACKNOWLEDGMENTS

This research was supported by an ERC Consolidator Grant (773121 NovelExperiSense) and by a Horizon GuestXR grant (101017884) (to A.A.). We thank Doctor Amber Maimon for helping with English language style.

AUTHOR CONTRIBUTIONS

D.-R.C., S.M., and A.A. conceived the experiments; D.-R.C. and S.M. performed the experiments; E.A.-V., D.-R.C., S.M., and A.A. wrote the manuscript; A.A. secured funding; S.M., D.-R.C., and A.A. developed the sensory substitution device and programmed its accompanying code as well as the experiment's graphic interfaces and data collection schemes; E.A.V. analyzed the data, performed analyses, and created preliminary figures; E.A.-V., D.-R.C., S.M., and A.A. interpreted the results and drafted the manuscript; E.-A.V., D.-R.C., and A.A. revised the manuscript.

DECLARATION OF INTERESTS

We had a patent on the EyeCane device. The patent is called "Infra-red based devices for guiding blind and visually impaired persons" (EP 2 496 196 B1). However, it is now expired as we could not pay the patent fees.

INCLUSION AND DIVERSITY

We support inclusive, diverse, and equitable conduct of research.

Received: July 16, 2022

Revised: November 23, 2022

Accepted: February 7, 2023

Published: April 10, 2023

REFERENCES

1. Pasqualotto, A., and Proulx, M.J. (2012). The role of visual experience for the neural basis of spatial cognition. *Neurosci. Biobehav. Rev.* **36**, 1179–1187.
2. Aggus-Vella, E., Kolarik, A.J., Gori, M., Cirstea, S., Campus, C., Moore, B.C.J., and Pardhan, S. (2020). Comparison of auditory spatial bisection and minimum audible angle in front, lateral, and back space. *Sci. Rep.* **10**, 6279.
3. Aggus-Vella, E., Campus, C., and Gori, M. (2017). Role of senses in representing portions of spaces around our body. *J. Vis.* **17**, 1050.
4. Aggus-Vella, E., Campus, C., Kolarik, A.J., and Gori, M. (2019). The role of visual experience in auditory space perception around the legs. *Sci. Rep.* **9**, 10992.
5. Milner, D., and Goodale, M. (2006). *The Visual Brain in Action* (OUP Oxford).
6. Hebart, M.N., and Hesselmann, G. (2012). What visual information is processed in the human dorsal stream? *J. Neurosci.* **32**, 8107–8109.
7. Pitzalis, S., Galletti, C., Huang, R.S., Patria, F., Committeri, G., Galati, G., Fattori, P., and Sereno, M.I. (2006). Wide-field retinotopy defines human cortical visual area V6. *J. Neurosci.* **26**, 7962–7973.
8. Galletti, C., Battaglini, P.P., and Fattori, P. (1995). Eye position influence on the parieto-occipital area PO (V6) of the macaque monkey. *Eur. J. Neurosci.* **7**, 2486–2501.
9. Helfrich, R.F., Becker, H.G.T., and Haarmeier, T. (2013). Processing of coherent visual motion in topographically organized visual areas in human cerebral cortex. *Brain Topogr.* **26**, 247–263.
10. Galletti, C., and Fattori, P. (2003). Neuronal mechanisms for detection of motion in the field of view. *Neuropsychologia* **41**, 1717–1727.
11. Galletti, C., and Fattori, P. (2018). The dorsal visual stream revisited: stable circuits or dynamic pathways? *Cortex* **98**, 203–217.
12. Fattori, P., Pitzalis, S., and Galletti, C. (2009). The cortical visual area V6 in macaque and human brains. *J. Physiol. Paris* **103**, 88–97.
13. Pitzalis, S., Fattori, P., and Galletti, C. (2013). The functional role of the medial motion area V6. *Front. Behav. Neurosci.* **6**, 91.
14. Pitzalis, S., Sereno, M.I., Committeri, G., Fattori, P., Galati, G., Patria, F., and Galletti, C. (2010). Human v6: the medial motion area. *Cereb. Cortex* **20**, 411–424.
15. Sulpizio, V., Galati, G., Fattori, P., Galletti, C., and Pitzalis, S. (2020). A common neural substrate for processing scenes and egomotion-compatible visual motion. *Brain Struct. Funct.* **225**, 2091–2110.
16. Tosoni, A., Pitzalis, S., Committeri, G., Fattori, P., Galletti, C., and Galati, G. (2015). Resting-state connectivity and functional specialization in human medial parieto-occipital cortex. *Brain Struct. Funct.* **220**, 3307–3321.
17. Hubel, D.H., and Wiesel, T.N. (1962). Receptive fields, binocular interaction and functional architecture in the cat's visual cortex. *J. Physiol.* **160**, 106–154.
18. Knudsen, E.I. (2004). Sensitive periods in the development of the brain and behavior. *J. Cogn. Neurosci.* **16**, 1412–1425.
19. Pascual-Leone, A., and Hamilton, R. (2001). The metamodal organization of the brain BT – Vision: from Neurons to Cognition. *Prog Brain Res.* **134**, 427–445.
20. Chebat, D.R., Schneider, F.C., and Ptito, M. (2020). Spatial competence and brain plasticity in congenital blindness via sensory substitution devices. *Front. Neurosci.* **14**, 815.
21. Ricciardi, E., Handjaras, G., and Pietrini, P. (2014). The blind brain: how (lack of) vision shapes the morphological and functional architecture of the human brain. *Exp. Biol. Med.* (Maywood) **239**, 1414–1420.
22. Kupers, R., Chebat, D.R., Madsen, K.H., Paulson, O.B., and Ptito, M. (2010). Neural correlates of virtual route recognition in congenital blindness. *Proc. Natl. Acad. Sci. USA* **107**, 12716–12721.

23. Frasnelli, J., Collignon, O., Voss, P., and Lepore, F. (2011). Crossmodal plasticity in sensory loss. *Prog. Brain Res.* 191, 233–249.
24. Striem-Amit, E., Dakwar, O., Reich, L., and Amedi, A. (2012). The large-scale organization of “visual” streams emerges without visual experience. *Cereb. Cortex* 22, 1698–1709.
25. Striem-Amit, E., Ovadia-Caro, S., Caramazza, A., Margulies, D.S., Villringer, A., and Amedi, A. (2015). Functional connectivity of visual cortex in the blind follows retinotopic organization principles. *Brain* 138, 1679–1695.
26. Sani, L., Ricciardi, E., Gentili, C., Vanello, N., Haxby, J.V., and Pietrini, P. (2010). Effects of visual experience on the human MT+ functional connectivity networks: an fMRI study of motion perception in sighted and congenitally blind individuals. *Front. Syst. Neurosci.* 4, 159.
27. Strnad, L., Peelen, M.V., Bedny, M., and Caramazza, A. (2013). Multivoxel pattern analysis reveals auditory motion information in MT+ of both congenitally blind and sighted individuals. *PLoS One* 8, e63198.
28. Striem-Amit, E., Almeida, J., Belledonne, M., Chen, Q., Fang, Y., Han, Z., Caramazza, A., and Bi, Y. (2016). Topographical functional connectivity patterns exist in the congenitally, prelingually deaf. *Sci. Rep.* 6, 1–13.
29. Lomber, S.G., Meredith, M.A., and Kral, A. (2010). Cross-modal plasticity in specific auditory cortices underlies visual compensations in the deaf. *Nat. Neurosci.* 13, 1421–1427.
30. Meredith, M.A., Kryklywy, J., McMillan, A.J., Malhotra, S., Lum-Tai, R., and Lomber, S.G. (2011). Crossmodal reorganization in the early deaf switches sensory, but not behavioral roles of auditory cortex. *Proc. Natl. Acad. Sci. USA* 108, 8856–8861.
31. Pavani, F., and Roder, B. (2012). Cross-modal plasticity as a consequence of sensory loss: insights from blindness and deafness. In *The New Handbook of Multisensory Processing* (MIT Press), pp. 737–759.
32. Pietrini, P., Furey, M.L., Ricciardi, E., Gobbini, M.I., Wu, W.H., Cohen, L., Guazzelli, M., and Haxby, J.V. (2004). Beyond sensory images: object-based representation in the human ventral pathway. *Proc. Natl. Acad. Sci. USA* 101, 5658–5663.
33. Chebat, D.R., Schneider, F.C., Kupers, R., and Ptito, M. (2011). Navigation with a sensory substitution device in congenitally blind individuals. *NeuroReport* 22, 342–347.
34. Heimler, B., Striem-Amit, E., and Amedi, A. (2015). Origins of task-specific sensory-independent organization in the visual and auditory brain: neuroscience evidence, open questions and clinical implications. *Curr. Opin. Neurobiol.* 35, 169–177.
35. Amedi, A., Hofstetter, S., Maidenbaum, S., and Heimler, B. (2017). Task selectivity as a comprehensive principle for brain organization. *Trends Cogn. Sci.* 21, 307–310.
36. Peelen, M.V., He, C., Han, Z., Caramazza, A., and Bi, Y. (2014). Nonvisual and visual object shape representations in occipitotemporal cortex: evidence from congenitally blind and sighted adults. *J. Neurosci.* 34, 163–170.
37. Heimler, B., and Amedi, A. (2020). Are critical periods reversible in the adult brain? Insights on cortical specializations based on sensory deprivation studies. *Neurosci. Biobehav. Rev.* 116, 494–507.
38. Chebat, D.R., Maidenbaum, S., and Amedi, A. (2017). The transfer of non-visual spatial knowledge between real and virtual mazes via sensory substitution. *Int. Conf. Virtual Rehabil. ICVR*, 1–7.
39. Kellogg, W.N. (1962). Sonar system of the blind. *Science* 137, 399–404.
40. Bassett, I.G., and Eastmond, E.J. (1964). Echolocation: measurement of pitch versus distance for sounds reflected from a flat surface. *J. Acoust. Soc. Am.* 36, 911–916.
41. Chebat, D.R., Maidenbaum, S., and Amedi, A. (2015). Navigation using sensory substitution in real and virtual mazes. *PLoS One* 10, e0126307.
42. Galletti, C., Fattori, P., Battaglini, P.P., Shipp, S., and Zeki, S. (1996). Functional demarcation of a border between areas V6 and V6A in the superior parietal gyrus of the macaque monkey. *Eur. J. Neurosci.* 8, 30–52.
43. Galletti, C., Fattori, P., Gamberini, M., and Kutz, D.F. (1999). The cortical visual area V6: brain location and visual topography. *Eur. J. Neurosci.* 11, 3922–3936.
44. Galletti, C., Gamberini, M., Kutz, D.F., Fattori, P., Luppino, G., and Matelli, M. (2001). The cortical connections of area V6: an occipito-parietal network processing visual information. *Eur. J. Neurosci.* 13, 1572–1588.
45. Pitzalis, S., Serra, C., Sulpizio, V., Committeri, G., de Pasquale, F., Fattori, P., Galletti, C., Sepe, R., and Galati, G. (2020). Neural bases of self- and object-motion in a naturalistic vision. *Hum. Brain Mapp.* 41, 1084–1111.
46. Galletti, C., Fattori, P., Gamberini, M., and Kutz, D.F. (2004). The most direct visual pathway to the frontal cortex. *Cortex* 40, 216–217.
47. Shipp, S., Blanton, M., and Zeki, S. (1998). A visuo-somatomotor pathway through superior parietal cortex in the macaque monkey: cortical connections of areas V6 and V6A. *Eur. J. Neurosci.* 10, 3171–3193.
48. Pitzalis, S., Sdoia, S., Bultrini, A., Committeri, G., Di Russo, F., Fattori, P., Galletti, C., and Galati, G. (2013). Selectivity to translational egomotion in human brain motion areas. *PLoS One* 8, e60241.
49. Pitzalis, S., Fattori, P., and Galletti, C. (2015). The human cortical areas V6 and V6A. *Vis. Neurosci.* 32, E007.
50. Pitzalis, S., Bozzacchi, C., Bultrini, A., Fattori, P., Galletti, C., and Di Russo, F. (2013). Parallel motion signals to the medial and lateral motion areas V6 and MT+. *Neuroimage* 67, 89–100.
51. Cardin, V., and Smith, A.T. (2010). Sensitivity of human visual and vestibular cortical regions to egomotion-compatible visual stimulation. *Cereb. Cortex* 20, 1964–1973.
52. Maidenbaum, S., Hanassy, S., Abboud, S., Buchs, G., Chebat, D.R., Levy-Tzedek, S., and Amedi, A. (2014). The “EyeCane”, a new electronic travel aid for the blind: technology, behavior & swift learning. *Restor. Neurol. Neurosci.* 32, 813–824.
53. Maidenbaum, S., Levy-Tzedek, S., Chebat, D.R., and Amedi, A. (2013). Increasing accessibility to the blind of virtual environments, using a virtual mobility aid based on the “EyeCane”: feasibility study. *PLoS One* 8, e72555.
54. Kobayashi, S., Ohashi, Y., and Ando, S. (2002). Effects of enriched environments with different durations and starting times on learning capacity during aging in rats assessed by a refined procedure of the Hebb-Williams maze task. *J. Neurosci. Res.* 70, 340–346.
55. Hebb, D.O., and Williams, K. (1946). A method of rating animal intelligence. *J. Gen. Psychol.* 34, 59–65.
56. Glasser, M.F., Coalson, T.S., Robinson, E.C., Hacker, C.D., Harwell, J., Yacoub, E., Ugurbil, K., Andersson, J., Beckmann, C.F., Jenkinson, M., et al. (2016). A multi-modal parcellation of human cerebral cortex. *Nature* 536, 171–178.
57. Serra, C., Galletti, C., Di Marco, S., Fattori, P., Galati, G., Sulpizio, V., and Pitzalis, S. (2019). Egomotion-related visual areas respond to active leg movements. *Hum. Brain Mapp.* 40, 3174–3191.
58. Zeharia, N., Hertz, U., Flash, T., and Amedi, A. (2012). Negative blood oxygenation level dependent homunculus and somatotopic information in primary motor cortex and supplementary motor area. *Proc. Natl. Acad. Sci. USA* 109, 18565–18570.
59. Zeharia, N., Hertz, U., Flash, T., and Amedi, A. (2015). New whole-body sensory-motor gradients revealed using phase-locked analysis and verified using multivoxel pattern analysis and functional connectivity. *J. Neurosci.* 35, 2845–2859.
60. Zeharia, N., Hofstetter, S., Flash, T., and Amedi, A. (2019). A whole-body sensory-motor gradient is revealed in the medial wall of the parietal lobe. *J. Neurosci.* 39, 7882–7892.
61. Pitzalis, S., Sereno, M.I., Committeri, G., Fattori, P., Galati, G., Tosoni, A., and Galletti, C. (2013). The human homologue of macaque area V6A. *Neuroimage* 82, 517–530.

62. Galletti, C., Gamberini, M., and Fattori, P. (2022). The posterior parietal area V6A: an attentionally-modulated visuomotor region involved in the control of reach-to-grasp action. *Neurosci. Biobehav. Rev.* **141**, 104823.
63. Galletti, C., Fattori, P., Kutz, D.F., and Gamberini, M. (1999). Brain location and visual topography of cortical area V6A in the macaque monkey. *Eur. J. Neurosci.* **11**, 575–582.
64. Becker, H.G.T., Haarmeier, T., Tatagiba, M., and Gharabaghi, A. (2013). Electrical stimulation of the human homolog of the medial superior temporal area induces visual motion blindness. *J. Neurosci.* **33**, 18288–18297.
65. Fischer, E., Bühlhoff, H.H., Logothetis, N.K., and Bartels, A. (2012). Human areas V3A and V6 compensate for self-induced planar visual motion. *Neuron* **73**, 1228–1240.
66. Schindler, A., and Bartels, A. (2018). Human V6 integrates visual and extra-retinal cues during head-induced gaze shifts. *iScience* **7**, 191–197.
67. Bach-y-Rita, P., and W Kercel, S. (2003). Sensory substitution and the human-machine interface. *Trends Cogn. Sci.* **7**, 541–546.
68. Bach-y-Rita, P. (2004). Tactile sensory substitution studies. In *Ann. N. Y. Acad. Sci.*, **1013** (New York Academy of Sciences), pp. 83–91.
69. Netzer, O., Heimler, B., Shur, A., Behor, T., and Amedi, A. (2021). Backward spatial perception can be augmented through a novel visual-to-auditory sensory substitution algorithm. *Sci. Rep.* **11**, 11944.
70. Ptito, M., Matteau, I., Gjedde, A., and Kupers, R. (2009). Recruitment of the middle temporal area by tactile motion in congenital blindness. *NeuroReport* **20**, 543–547.
71. Ptito, M., Matteau, I., Zhi Wang, A., Paulson, O.B., Siebner, H.R., and Kupers, R. (2012). Crossmodal recruitment of the ventral visual stream in congenital blindness. *Neural Plast.* **2012**, 304045.
72. Collignon, O., Champoux, F., Voss, P., and Lepore, F. (2011). Sensory rehabilitation in the plastic brain. *Prog. Brain Res.* **191**, 211–231.
73. Karnath, H.O., and Rorden, C. (2012). The anatomy of spatial neglect. *Neuropsychologia* **50**, 1010–1017.
74. Halligan, P.W., Fink, G.R., Marshall, J.C., and Vallar, G. (2003). Spatial cognition: evidence from visual neglect. *Trends Cogn. Sci.* **7**, 125–133.
75. Jacobs, J., Korolev, I.O., Caplan, J.B., Ekstrom, A.D., Litt, B., Baltuch, G., Fried, I., Schulze-Bonhage, A., Madsen, J.R., and Kahana, M.J. (2010). Right-lateralized brain oscillations in human spatial navigation. *J. Cogn. Neurosci.* **22**, 824–836.
76. Fries, P., Nikolić, D., and Singer, W. (2007). The gamma cycle. *Trends Neurosci.* **30**, 309–316.
77. Jensen, O., Kaiser, J., and Lachaux, J.P. (2007). Human gamma-frequency oscillations associated with attention and memory. *Trends Neurosci.* **30**, 317–324.
78. Lachaux, J.P., Fonlupt, P., Kahane, P., Minotti, L., Hoffmann, D., Bertrand, O., and Bacia, M. (2007). Relationship between task-related gamma oscillations and BOLD signal: new insights from combined fMRI and intracranial EEG. *Hum. Brain Mapp.* **28**, 1368–1375.
79. Mukamel, R., Gelbard, H., Arieli, A., Hasson, U., Fried, I., and Malach, R. (2005). Coupling between neuronal firing, field potentials, and fMRI in human auditory cortex. *Science* **309**, 951–954.
80. Logothetis, N.K., Pauls, J., Augath, M., Trinath, T., and Oeltermann, A. (2001). Neurophysiological investigation of the basis of the fMRI signal. *Nature* **412**, 150–157.
81. Pitzalis, S., Serra, C., Sulpizio, V., Di Marco, S., Fattori, P., Galati, G., and Galletti, C. (2019). A putative human homologue of the macaque area PEc. *Neuroimage* **202**, 116092.
82. Amedi, A., Merabet, L.B., Bermpohl, F., and Pascual-Leone, A. (2005). The occipital cortex in the blind: lessons about plasticity and vision. *Curr. Dir. Psychol. Sci.* **14**, 306–311. <https://doi.org/10.1111/j.0963-7214.2005.00387.x>.
83. Amedi, A., Malach, R., Hendler, T., Peled, S., and Zohary, E. (2001). Visuo-haptic object-related activation in the ventral visual pathway. *Nat. Neurosci.* **4**, 324–330.
84. Ricciardi, E., Vanello, N., Sani, L., Gentili, C., Scilingo, E.P., Landini, L., Guazzelli, M., Bicchieri, A., Haxby, J.V., and Pietrini, P. (2007). The effect of visual experience on the development of functional architecture in hMT+. *Cereb. Cortex* **17**, 2933–2939.
85. Ricciardi, E., Papale, P., Cecchetti, L., and Pietrini, P. (2020). Does (lack of) sight matter for V1? New light from the study of the blind brain. *Neurosci. Biobehav. Rev.* **118**, 1–2.
86. Poirier, C., Collignon, O., DeVolder, A.G., Renier, L., Vanlierde, A., Tranduy, D., and Scheiber, C. (2005). Specific activation of the V5 brain area by auditory motion processing: an fMRI study. *Brain Res. Cogn. Brain Res.* **25**, 650–658.
87. Wiesel, T.N., and Hubel, D.H. (1963). Single-cell responses in striate cortex of kittens deprived of vision in one eye. *J. Neurophysiol.* **26**, 1003–1017.
88. Wiesel, T.N., and Hubel, D.H. (1965). Comparison of the effects of unilateral and bilateral eye closure on cortical unit responses in kittens. *J. Neurophysiol.* **28**, 1029–1040.
89. Lewis, T.L., and Maurer, D. (2005). Multiple sensitive periods in human visual development: evidence from visually deprived children. *Dev. Psychobiol.* **46**, 163–183.
90. Birch, E.E., Cheng, C., Stager, D.R., Weakley, D.R., and Stager, D.R. (2009). The critical period for surgical treatment of dense congenital bilateral cataracts. *J. AAPOS Off. Publ. Am. Assoc. Pediatr. Ophthalmol. Strabismus* **13**, 67–71.
91. Dormal, G., Lepore, F., and Collignon, O. (2012). Plasticity of the dorsal “spatial” stream in visually deprived individuals. *Neural Plast.* **2012**, 687659.
92. Maidenbaum, S., Levy-Tzedek, S., Chebat, D.R., Namer-Furstenberg, R., and Amedi, A. (2014). The effect of extended sensory range via the eyecane sensory substitution device on the characteristics of visionless virtual navigation. *Multisens. Res.* **27**, 379–397.
93. Meunier, M., Saint-Marc, M., and Destrade, C. (1986). The Hebb-Williams test to assess recovery of learning after limbic lesions in mice. *Physiol. Behav.* **37**, 909–913.
94. Zimmermann, R.R. (1969). Performance of baby monkeys on the Hebb-Williams closed field maze learning task. *Dev. Psychobiol.* **2**, 40–42.
95. Shore, D.I., Stanford, L., MacInnes, W.J., Klein, R.M., and Brown, R.E. (2001). Of mice and men: virtual Hebb-Williams mazes permit comparison of spatial learning across species. *Cogn. Affect. Behav. Neurosci.* **1**, 83–89.
96. RStudio (2011). RStudio: integrated development environment for R75, Version 0.97.311 (J. Wildl. Manage), pp. 1753–1766.
97. Benjamini, Y., and Hochberg, Y. (1995). Controlling the false discovery rate: a practical and powerful approach to multiple testing. *J. R. Stat. Soc. B* **57**, 289–300.
98. Frost, M.A., and Goebel, R. (2012). Measuring structural-functional correspondence: spatial variability of specialised brain regions after macro-anatomical alignment. *Neuroimage* **59**, 1369–1381.
99. Thiebaut de Schotten, M., Ffytche, D.H., Bizzi, A., Dell’Acqua, F., Allin, M., Walshe, M., Murray, R., Williams, S.C., Murphy, D.G.M., and Catani, M. (2011). Atlasing location, asymmetry and inter-subject variability of white matter tracts in the human brain with MR diffusion tractography. *Neuroimage* **54**, 49–59.
100. Bartolomeo, P., and Seidel Malkinson, T. (2019). Hemispheric lateralization of attention processes in the human brain. *Curr. Opin. Psychol.* **29**, 90–96.
101. Collignon, O., Vandewalle, G., Voss, P., Albouy, G., Charbonneau, G., Lassonde, M., and Lepore, F. (2011). Functional specialization for auditory-spatial processing in the occipital cortex of congenitally blind humans. *Proc. Natl. Acad. Sci. USA* **108**, 4435–4440.
102. Herbet, G., Yordanova, Y.N., and Duffau, H. (2017). Left spatial neglect evoked by electrostimulation of the right inferior fronto-occipital Fasciculus. *Brain Topogr.* **30**, 747–756.

STAR★METHODS

KEY RESOURCES TABLE

REAGENT or RESOURCE	SOURCE	IDENTIFIER
Deposited data		
Data and Code		https://doi.org/10.5281/zenodo.7574391
Software		
Brainvoyager	Brain Innovation	https://www.brainvoyager.com/
Rstudio	Cran r project	https://www.r-project.org/

RESOURCE AVAILABILITY

Lead contact

Further clarifications or request will be attended by the lead contact author Amir Amedi (amir.amed@idc.ac.il).

Materials availability

This study did not generate any unique reagents.

Data and code availability

Data are available on zenodo <https://doi.org/10.5281/zenodo.7574391>

EXPERIMENTAL MODEL AND SUBJECT DETAILS

Twenty-three participants participated in this study, fourteen sighted participants who performed the task using vision (8 women, range: 19–55 years, average: 28 years, mode: 21 years), and nine congenitally blind (CB) participants (3 women, range: 23–59 years, average: 36 years, mode: 23 years). Blindness was peripheral in all cases (i.e., not due to brain injury), see Table. All CB participants were adept white cane users and had previously received training in orientation and mobility. The two sample sizes were estimated through power analysis, taking an estimate of effect size from a subsample of 3 participants for each group separately with the desired power of .80 and alpha of .05. We estimated a minimum of 10 blind participants and 8 sighted participants. Nineteen sighted participants participated in the body motor task. This experiment was approved by the Hebrew University's ethics committee and conducted in accordance with the 1964 Helsinki Declaration and complies with all relevant ethical regulations. All participants signed informed consent forms prior to the start of the study and were compensated for their time.

Demographics of the congenitally blind participants

Name	Age	Sex	Onset	Light perception	Cause of blindness
D.A.	59	M	birth	none	retinopathy of prematurity
M.D.	23	M	birth	none	congenital glaucoma
U.M.	41	M	6–7 months	none	retinopathy of prematurity
O.B.	38	M	birth	none	retinopathy of prematurity
O.G.	38	F	birth	none	anophthalmia
E.D.	33	M	birth	none	retinopathy of prematurity
E.H.	30	F	birth	faint	retinopathy of prematurity
E.N.	30	F	birth	none	anophthalmia
M.S.	37	F	birth	none	anophthalmia

METHOD DETAILS

Navigation task

The task was to find the fastest route to the exit while avoiding collisions (touching) the walls. Participants stood at the entrance of the maze and held the EyeCane (see EyeCane section), while wearing headphones that transmitted the distance information based on the EyeCane's cues. They were informed that the distance to walls was coded in terms of the frequency of the sound, the further away the wall was the lower was the frequency of the sound and that the absence of sound meant that the passage was clear. Participants were instructed to use the EyeCane to scan the environment and build a mental image of the maze to find the shortest route to the exit. In the virtual version of the mazes, participants were seated comfortably in front of the computer, wearing headphones and received the distance information based on the same low/high rate of auditory cues. Participants navigated with the help of the arrow keys on the keyboard. The forward arrow key enabled a step forward, the right arrow key a turn to the right and the left arrow key a turn to the left. The sighted group was instructed on the task prior to scanning. They only performed a single scan because they did not require training as they were allowed to use vision. The blind group underwent two scans, one before, and one after the training sessions between scans spread out over a three-day period to learn to use the EyeCane. For a description of the training procedure see ^{38,41}.

The EyeCane device (Figure 1C) is an in-house minimalistic sensory substitution device, translating distance into auditory cues in real-time⁵². It has already been used for several other tasks.^{52,92} We created a virtual version of the EyeCane,⁵³ providing auditory cues in virtual reality training, identical to those presented in the real-world. The virtual version of the EyeCane uses a ray-casting algorithm within the virtual environment. Both, the EyeCane and virtual EyeCane send a high frequency of sound when an object is near and a low frequency when objects are far away. This enables the user to detect distance information in the form of sound frequency. Spatial information is perceived by scanning the environment in the same way that a white cane is used. This sweeping motion, which in the real world was performed by sweeping it around to scan the environment more freely, was slightly more confined to only 3 directions of pointing the cane in the virtual world – left, right or straight ahead. This enables the construction of a mental representation of the user's surroundings. In order to "sweep" the virtual EyeCane left and right, they would press the left and right arrow keys, but without moving forward. When the EyeCane was silent, or "quieter" in terms of the frequency of sounds, it meant the wall was further away, so they would advance. We chose this interface because if participants could move their "gaze" to point in one direction, but have the avatar facing another direction, they would not be able to know which direction their avatar was facing. This design feature is critical for the study as it allows to test the hypothesis of the study.

The virtual navigation setup

The mazes (Figures 1D and 1E) were based on the classic Hebb-Williams mazes,⁵⁵ which have been previously used for testing spatial perceptual learning in a wide variety of species, from mice⁹³ to non-human primates,⁹⁴ and even in a virtual rendition for humans.⁹⁵ Our virtual environments⁵³ were created with Blender 2.49, and Python 2.6.2. The location and orientation of the user's avatar and virtual EyeCane were tracked at all times at a rate of 60 Hz (identical to the function rate of the virtual environment, thus covering any possible in-game activity) and were aligned via logged triggers to the neural data. The environments have a graphical output to the screen, which was used by the sighted group. The participants always experienced the environments in the first person, and the virtual mazes perfectly matched the real-world mazes used in training with relation to spatial layout. Distances within the environment were set so that each "virtual meter" correlates to a real-world meter (i.e., the real-world maze was 4.5m, so the virtual maze was set to 4.5 virtual meters), with the same holding for the scale of avatar size and motion. Distances within the environment are set so that the proportions of a step compared to a "virtual meter" correlates to a real-world step compared to a meter (i.e. the real world maze was 4.5m, so the virtual maze was set to 4.5 virtual meters, as was the scale of the avatar's size and motion; each step measured 0.5 virtual meters).

Design (Table S1): Prior to any training, CB participants were scanned using fMRI while performing the 2 Hebb-Williams mazes and the scrambled condition. Then, CB participants were trained on 1 maze (the maze 1 training) for three sessions using the EyeCane and the virtual EyeCane. In each of the three training sessions, participants completed the Hebb-Williams maze five times in the real environment. Then, they were instructed to navigate the virtual maze. On the second and third session, participants returned and repeated the same sequence of five real maze and five virtual mazes. Each session lasted ninety minutes to two hours. After the three training sessions, CB participants returned for a second fMRI session. The sighted-visual control group did the exact same task in fMRI with the use of vision in one single block of five trials that lasted less than one hour. The methods and behavioral results have been described in depth in Chebat et al..⁴¹

Body motor task

For the motor task, participants were required to move 20 body parts in a fixed order.⁶⁰ The movement sequence consisted of the movements of the following body parts: toes (flexion/extension), feet (flexion/extension), thighs (contraction), buttocks (contraction), stomach (contraction), upper arm (contraction), elbow (flexion/extension), wrist (flexion/extension), fist (contraction), little finger (flexion/extension), ring finger (flexion/extension), middle finger (flexion/extension), index finger (flexion/extension), thumb (flexion/extension), forehead (contraction), nose (contraction), eyelids (contraction), lips (contraction), jaw (flexion/extension), and tongue (a side to side movement with closed mouth).

Tasks inside the scanner

Magnetic Resonance Imaging Navigation.

In the scanner, participants underwent 8 repetitions of three conditions:

- 1 Maze 1 training- A virtual recreation of Hebb-William's maze A (Figure 1D), on which participants **were** trained between the pre and post scans
- 2 Maze 2 no training- A virtual recreation of Hebb-William's maze B (Figure 1E), on which participants **were not** trained
- 3 Scrambled – Controlled for auditory stimuli and motor key presses without actual navigation via scrambled visual and auditory stimuli from the mazes, Participants were told to move normally by pressing the keystrokes.

The participants included in the study showed no translational motion exceeding 2 mm in any given axis or had spike-like motion of more than 1 mm in any direction.

Magnetic Resonance Imaging body motor. A periodic design experiment^{58,59} was used to inspect body information in area V6. In this experiment, 19 sighted participants were asked to move 20 body parts separately. The 20 body parts were moved consecutively in a fixed order (from toes to tongue or in reversed order). The participants were instructed to execute the movements on hearing an auditory cue. Each body part was moved for 3 s, and the movement cycle, consisting of movements of all 20 body parts, was followed by 12 s rest and it was repeated eight times in each direction (toes to tongue and tongue to toes). The movements were either synchronized in-phase bilateral movements (e.g., concurrent movements of the toes on the left and right feet) or axially symmetric body part movements (e.g., side-to-side movements of the tongue). Participants moved the 20 body parts consecutively while lying with their eyes closed and blindfolded inside the functional MRI scanner. Electromyographic (EMG) signals were recorded during the scan in several participants to ensure that the movements were correctly carried out and exclude the possibility of movement of other body parts. The maximum value of head movements was 2.46 mm (in the order of magnitude of one functional voxel; i.e., relatively negligible head motion), and the mean was 0.21 ± 0.28 mm

Functional parameters

Navigation task. The BOLD fMRI measurements were acquired in a whole-body 3T GE Sigma scanner (GE Medical Systems, USA). We used the standard gradient-echo EPI pulse sequence. We acquired 27 slices of 4.5 mm thickness and 0 mm gap. The data in-plane matrix size was 64X64, field of view (FOV) 220 mm 220 mm, time to repetition (TR) 1.5s, flip angle $\frac{1}{4}$ 70 and TE 35 ms. The first 10 images of each scan were excluded from the analysis because of non-steady-state magnetization.

Body motor task. The BOLD fMRI measurements were obtained in a whole-body 3T Magnetom Trio scanner with 12 channels (Siemens). The fMRI protocols were based on multi slice gradient echoplanar imaging and a standard head coil. The functional data was collected under the following timing parameters: TR = 1.5 s; TE = 30 ms; FA = 70°; imaging matrix, 80 × 80; FOV, 24 × 24 cm (i.e., in-plane resolution of 3 mm). We used a relatively short TR value to later superimpose the phase-locking spectral analysis (cross correlation) approach. Twenty-six slices with slice thickness of 4.5 mm and no gaps were oriented in the axial position for complete coverage of the cortex. Given that the slice thickness was higher than the in-plane resolution, the spatial resolution along the dorsoventral, superior-inferior axis was lower than the resolution along the posterior-anterior and medial-lateral axes.

Preprocessing

Navigation task. The fMRI image processing and statistical analyses were performed with the BrainVoyager 20.6 and 21.4 software package (Brain Innovation, Maastricht), using standard preprocessing procedures, including head-motion correction, slice scan-time correction, high-pass filtering. Functional and anatomical datasets of each participant were normalized to standardized MNI space. Cortical reconstruction included segmentation of white matter using a grow-region function, the remaining cortical surface was then inflated and aligned to a 3D cortical reconstruction of an MNI normalized brain (FreeSurfer's fs Average brain).

Body motor task. The first 10 images (during the first baseline rest condition) were excluded from the analysis in both designs (toes to tongue and tongue to toes) because of non-steady-state magnetization. Data was preprocessed using the BrainVoyager software package (Brain Innovation). Functional MRI data preprocessing included head-motion correction, slice scan time correction and high-pass filtering using temporal smoothing in the frequency domain removed drifts and improved the signal-to-noise ratio. Cortical reconstruction included segmentation of white matter using a grow-region function, the remaining cortical surface was then inflated and aligned to a 3D cortical reconstruction of an MNI normalized brain (FreeSurfer's fs Average brain).

QUANTIFICATION AND STATISTICAL ANALYSIS

Navigation task

We performed ROI analysis on the reconstructed and inflated fsAverage brain to which we aligned all participants' brains with cortex-based alignment procedure. We computed statistical parametric maps from a single participant General Linear Model (GLM). Predictors in the model were convoluted with a canonical Hemodynamic Response Function. For the group-level analysis, we ran a random-effects GLM model in each POI-ROI: anatomical V6, V6A, DVT and A1. The beta value of each participants, session, and condition, was then extracted and imported into R software⁹⁶ for further analysis. Multiple comparison two tails t-tests were FDR corrected with $p < 0.05$,⁹⁷ while t values are reported with no correction.

Navigation task. Regions of interest (ROI) analysis

Four anatomical ROIs were defined by aligning every single participant's brain to the Glasser atlas using the CBA approach (it is crucial to keep in mind that we didn't project the results from volume to a surface brain where the atlas is built but we performed the cortex based alignment that means to align every sulcus and gyrus of each hemisphere of each participant to the surface brain on which the atlas was built and we performed the analysis only in surface space. General linear model (GLM) analysis was performed in each of the 4 anatomical ROIs defined by the Glasser atlas (V6, A1, V6A and DVT) yielding the GLM parameter estimators for each of the three conditions (both mazes and the scramble condition). We used BrainVoyager to calculate GLM parameters estimation values, while multiple t-test comparisons were performed in R studio software.⁹⁶

Body motor task

The cyclic design of the periodic experiment allowed for periodic analysis, which is considered optimal for analyzing gradual topographic representations. We used the cross-correlation analysis, similar to the spectral analysis, but in which the HRF is still considered. In the cross-correlation analysis, the hemodynamic response function (HRF) predictor, corresponding to the movement time of a single body part, was cross-correlated with the BOLD signal. However, this predictor makes the cross-correlation analysis highly sensitive to the shape of the response and the degree of overlap in representation. Given that the HRF predictor corresponds to the movement time of a single body part, this analysis is suitable when the overlap in representation is small but less adequate when the voxel is broadly tuned to movements of various body parts. This analysis is a winner takes all analysis, meaning that only one lag value corresponding to only one body part is chosen for each vertex-voxel. This result may allow a clear estimation of the represented body part in each voxel but as stated above, is less optimal in cases of some overlap in the representation. (see Zeharia et al.⁵⁸ for details). We applied full brain cross-correlation analysis and correct each single participant map with FDR (R equal to 0.219). To investigate if area V6 contains body info, we extracted V6 details (Vertex ID, coordinates and the associated R and P values) from the full brain cross correlation already corrected with FDR (R equal to 0.219). Only vertices with significant P, after the full brain correction, were considered. The 20 body parts were grouped in 3 anatomy-based sections: Low body parts (Toes, Feet, Hips, Buttocks and Stomach), Upper body part (Arm, Elbow, Wrist, Fist plus the 5 fingers) and Head (Forehead, nose, eyes, Lips, Jaw, Tongue). T-test versus baseline was used to test body information inside the V6 area. Then, multiple comparison t-test was performed on these 3 body sections and corrected with FDR correction.

Body motor task ROI mask

Full brain cross correlation of each participant, corrected with FDR was masked with four ROI: V6, V6A, MT and area 4. These 4 ROIs were defined using the same procedure used for the navigation task (CBA to freesurfer brain on which the Glasser atlas is mapped).

Both experiments

Cortex based alignment (CBA)

To extract precise anatomical markers as regions of interest (ROI) we used a cortex-based alignment (CBA) algorithm implemented in BrainVoyager.⁹⁸ Functional and anatomical files from each experiment were aligned to a fsAverage brain surface. This approach has the goal of improving the spatial correspondence mapping between participants' brains beyond MNI space matching. In short, the process morphs reconstructed and folded hemispheres into a sphere that produces a curvature map with differing degrees of smoothness. The alignment itself is an iterative procedure that follows a coarse-to-fine matching strategy to a target brain that gradually decreases the smoothness of the sphere's surface. We aligned and analyzed each hemisphere in isolation. Spatial tasks were found to be processed mostly in the right hemisphere,^{99,100} indeed, studies on patients with right brain damage showed a predominant spatial deficit, while spatial deficit, after left brain injury, are less common. This evidence led to think a predominant role of the right hemisphere in spatial tasks,^{73,74,101} but see Herbet et al.¹⁰²

All the functional datasets, at first created in a standard MRI volume space, were then aligned to the target surface. The final resolution was 80K vertices and 81920 triangles.

Roi definition

The CBA procedure allowed us to align every participants' brain to the same template on which the HCP atlas/parcellation was defined.⁵⁶ This procedure has the advantage of taking into account intrasubject differences, as it is based on a big sample (210) of participants and, so, it enhances anatomical localization. This method is very powerful for study replication, as it takes into account intrasubject variability/bias, allowing the use of the same area across different groups in the world. In this study, we focused on the V6 area (Figure 2), as an important area for navigation. In addition to V6, in order to control for auditory differences between conditions, we analyzed activation in the anatomical auditory cortex (A1). Furthermore, we analyzed closer areas to area V6, as V6A and area DVT. For the motor task, we investigated area 4 and area MT as control areas.

Atlas details

The Glasser atlas is an atlas brain developed using probability maps from 210 participants, then combined to produce a group maximum probability map (MPM). Each area of each probabilistic map was defined based on its multi-modal fingerprints. Specifically, the Glasser atlas is defined by sharp changes in cortical architecture, function, connectivity, and/or topography in a precisely aligned group average of 210 healthy young adults. Area V6 was defined by using topographic information from rfMRI FC. The Glasser atlas differentiated area V6 from area V6A based on myelination and tasks data " Areas V6 and V6A lie mainly medial and anterior to areas V2, V3, V3A, and V7 along the posterior bank of the parieto-occipital sulcus and have been studied

extensively^{7,13,48,50,61}. V6 is heavily myelinated relative to most of its neighbors (particularly V6A and DVT, the dorsal transitional visual area). Relative to its superior neighbor V6A, area V6 is weakly activated vs weakly deactivated in the Working Memory contrast (2BK-0BK), and less deactivated in the MOTOR AVG contrast". Since we could not run a functional localizer in the CB group, we deemed this approach to be sufficiently reasonable and quite powerful as it is based on a very large sample (210 participants), while our sighted group was composed of 14 participants. However, Glasser V6 and V6A are very close to areas V6 and V6A as defined by Pitzalis.^{48,61} (Figure S2)

Statement on ethical regulations

These experiments were approved by the Hebrew University's ethics committee and conducted in accordance with the 1964 Helsinki Declaration and complies with all relevant ethical regulations. All participants signed informed consent forms prior to the start of the study and were compensated for their time.